



Improving the flame-retardant property of bottle-grade PET foam made by reactive foam extrusion

Christian Bethke¹ | Daniela Goedderz^{2,3} | Lais Weber^{2,3} | Tobias Standau¹ |
Manfred Döring² | Volker Altstädt¹

¹Department of Polymer Engineering, University of Bayreuth, Bayreuth, Germany

²Fraunhofer Institute for Structural Durability and System Reliability LBF, Darmstadt, Germany

³Ernst-Berl Institute for Chemical Engineering and Macromolecular Science, Technische Universität Darmstadt, Darmstadt, Germany

Correspondence

Volker Altstädt, Department of Polymer Engineering, University of Bayreuth, Universitätsstraße 30, 95447 Bayreuth, Germany.

Email: altstaedt@uni-bayreuth.de

Funding information

Research Foundation

Abstract

Upcycling of low intrinsic viscosity (IV) poly(ethylene terephthalate) (PET) grades, such as bottle- or recycled grades, by a reactive foam extrusion process, provides an appropriate alternative to high pricing, high IV grades commonly used for foaming applications. However, the drawback of bottle-grade PET foams is its flame retardant (FR) performance. In this study, pyromellitic dianhydride was used as a chain extender to foam bottle-grade PET. The influence of different FRs, containing halogenated (HFR) and four different phosphorous-based types, on the processability and final foam properties was investigated. HFR showed better processability to achieve proper foams with fine morphology compared to P-based FRs, where the FR content was adjusted between 2 and 5 wt%. However, HFR exhibited lower FR performance by cone calorimeter testing compared to the P-based FRs and the commercial reference foam Kerdyn. Nonetheless, all of the FRs can only improve the time to ignition of the neat PET foams while the other values depend on the specific type of FR. In addition, all FR foams have improved mechanical properties more than twice in comparison to the neat PET foam.

KEYWORDS

cone calorimetry, flame retardant, mechanical properties, PET, reactive foam extrusion

1 | INTRODUCTION

Polymeric foams are favorable in modern engineering, as they combine lightweight, along with material saving, low thermal conductivity, and high specific mechanical performance. These properties make polymeric foams particularly suitable for packaging, construction, and transportation industries. Their properties are adaptable to a wide range of specific applications. Therefore, its basic polymer, its processing route, the resulting foam morphology, and density have to be considered. Besides

bead foaming technology, foam extrusion is one of the favorite processing routes when high output rates are demanded. Examples for polymers commonly used for foam extrusion are polystyrene, polyvinyl chloride, polyethylene, polypropylene, and poly(ethylene terephthalate) (PET).^[1] Among the polymer foams, PET provides beneficial aspects such as good solvent resistance, high elastic moduli and impact resistance, as well as high thermal stability and service temperature (T_g).^[1] Extruded PET foams and PET bead foams are commercially available from CoreLite Inc. (CoreLite PET Florida, United

This is an open access article under the terms of the Creative Commons Attribution License, which permits use, distribution and reproduction in any medium, provided the original work is properly cited.

© 2020 The Authors. *Journal of Applied Polymer Science* published by Wiley Periodicals, Inc.

States), Armacell Benelux S.A. (ArmaFORM PET, Arma-Shape, Thimister-Clermont, Belgium), Gurit (Kerdyn), Wattwil, Switzerland, DIAB Group (Divinycell), Helsingborg, Sweden, and 3A Composites (AIREX), Sins, Switzerland. However, it is typically known for polyesters like PET that foaming is challenging due to the low melt strength of common PET and PBT types leading to an unflattering cellular morphology.^[2-7]

Next to the optimization of processing equipment and parameters, the increase of the melt strength by chemical modification was found to be beneficial to overcome these issues, even for recycled PET. Therefore, favorably multifunctional additives act as chain extenders (CEs) and can be added to the polymer melt during the extrusion process in order to initiate a chemical reaction between multiple polymer chains. These CEs have to fulfill specific requirements such as high availability, sufficient thermal stability, and fast reaction without byproducts.^[8] Meanwhile, there are various numbers of CEs in the focus of research such as multifunctional epoxies, bis-oxazolines, dianhydrides, and diisocyanates. Thereof, epoxy-based or dianhydride-based tetrafunctional CEs revealed as most effective for PET foam extrusion.^[1,9-11] The intrinsic viscosity (IV) can often be found as an indicator for processability, as it can be correlated to the molecular weight and the hydrodynamic volume of the polymer chain. In general, high IV grades are favorable for foaming processes as low amounts or even no CEs are required for foaming. However, a study of Xanthos et al. revealed that the IV grades have to be seen relative with regards to foamability. They investigated different PET resins with an IV grade between 0.7 and 1.0 dL g⁻¹ of neat resins with poor foamability. In contrast, modified PET grades with an IV grade between 0.87 and 0.95 dL g⁻¹ performed well.^[12] This can be explained to the lack of appropriate information about branched structures in the IV value, which significantly contributes to melt elasticity and the foaming process.^[4]

As the market for polymer foams is rising, the fire safety performance of combustible organic polymers gains more significance. The flame retardant (FR) system has to be tailored for each polymer system and application in order to obtain the best performance. FRs for polyesters require high thermal stabilities of up to 280°C during the processing step and should have no significant influence on the melt viscosity. There are numerous FRs that fulfill these requirements and are suitable for the foam extrusion with PET.^[13] However, established halogenated FR types have to be replaced due to upcoming regulations.^[14,15] Thus, current researches are focusing on inorganic- and phosphorous-based FRs.^[16-18]

As inorganic FRs are used in high filler content for effective results, the foam density is influenced

negatively. Thus, phosphorous-based (P-based) FRs are more suitable when lightweight is a crucial factor.

To the best of the author's knowledge, no complete studies for the development process of FR bottle-grade PET foams made by reactive foam extrusion can be found in literature. Within this work, the influence of the different types of FRs, halogenated and P-based, on the reactive foam extrusion process of a bottle-grade PET with PMDA is studied. In addition, the basic morphological, mechanical, and FR properties of the resulting foams are presented. Therefore, a low IV (and thus low molecular weight) bottle-grade PET is processed by reactive foam extrusion with PMDA as CE and different commercially available FR in order to investigate the influence of the FRs on the foaming process and resulting foam properties. A halogen-containing flame retardant (HFR), a phosphinate salt (DEPZn), a phosphonate (PSMP), and a mixed phosphonate/phosphate (DOP) containing FR are used to compare characteristic material properties of the resulting PET foams regarding their foaming processability, mechanical performance, fire behavior, and thermal material properties. Next to basic material characteristics, such as glass transition (T_g), melt temperature (T_m), and molecular weights (M_n and M_w), the resulting foam properties with regard to density and morphology are of interest. Therefore, the foam density, cell size, and cell distribution are investigated. Additionally, the mechanical performance of the foams in compression and three-point bending is studied. Finally, cone calorimetry and single-flame source tests were used to investigate the fire, smoke and toxicity (FST) behavior. The material characteristics were modified to enable the foaming of low IV grade PET. The different FRs were successfully introduced in the foaming process. The resulting foams own applicable properties compared to the reference PET foam system.

2 | EXPERIMENTAL SECTION

2.1 | Materials

Table 1 summarizes the composition of the different investigated foam samples. A low viscosity bottle-grade PET resin AQUA NeopET 76 (Neo Group, Rimkai, Lithuania) with an IV of 0.76 dL g⁻¹, T_m 248°C, and a density of 1.34 g cm⁻³ was used. Pyromellitic dianhydride (PMDA) (Sigma Aldrich, St. Louis, MO) was used as a CE for PET in specified ratios. The blowing agent CO₂ was supplied with a purity grade of 4.5 (Rießner Gase, Lichtenfels, Germany). Three phosphorous-based FRs were used: (a) Zinc diethyl phosphinate, supplied as Exolit OP950 (Clariant, Muttenz, Switzerland), further named DEPZn.

TABLE 1 Overview of PET foam samples, its chain extender (PMDA), and flame retardant (FR) content by wt%

Sample	PMDA (wt%)	FR (wt%)	T_D (°C)	T_M (°C)	p_D (bar)	Density	Density	PDI
						sd. (g L ⁻¹)	Cal. (g L ⁻¹)	
Unfoamed PET	–	–	–	–	–	–	–	1.70
CE-PET V1	0.25	0	255	254	100 ± 5	105 ± 5	157 ± 8	3.31
CE-PET V2	0.33	0	245	250	110 ± 5	89 ± 1	253 ± 9	2.86
5 wt% DEPZn	0.35	5	255	250	100 ± 5	105 ± 2	193 ± 8	3.18
5 wt% HFR	0.25	5	250	255	105 ± 5	95 ± 2	253 ± 24	3.05
3 wt% PSMP	0.35	3	255	250	70 ± 10	132 ± 10	401 ± 78	3.12
2 wt% PSMP ^a	0.40	2	240	247	115 ± 5	93 ± 4	221 ± 16	2.78
2 wt% DOP	0.35	2	245	248	75 ± 5	91 ± 4	245 ± 16	2.67
KD ^b	–	–	–	–	–	–	190 ± 15	3.51

The extrusion parameters regarding the die (T_D) and melt (T_M) temperature, as well as the pressure at the die (p_D), are stated. Additionally, the resulting foam density before (Density sd.) and after the calibration process (Density cal.) is presented, as well as the polydispersity index (PDI).

^aContains ZnSt in a 20:1 ratio PSMP:ZnSt.

^bCommercial reference system.

(b) 6H-dibenz[c,e] [1,2]oxaphosphorin,6-[(1-oxido-2,6,7-trioxa-1-phosphabicyclo[2.2.2]oct-4-yl)methoxy]-, 6-oxide (DOPO-O-PEPA) supplied as DOPO-O-PEPA (Metadynea, Krems, Austria), further named DOP. (3) Pentaerythritol spirosbis(methylphosphonate), supplied as AFLAMMIT PCO 910 (THOR, Speyer, Germany), further named PSMP. To improve the processability during the foam extrusion process, one of the samples containing PSMP was prepared containing a mixture of PSMP and zinc stearate (ZnSt) (Sigma Aldrich) in a ratio PSMP:ZnSt = 20:1. As HFR, 1,2-Bis(tetrabromophthalimido ethane), further named HFR, supported as Saytex BT-93 (Albemarle, Charlotte, NC), was used. The chemical structures of the FRs used are shown in Figure 1.

All additives were dried under vacuum at 50°C for at least 24 h before processing.

The commercially available and flame-retardant PET foam Kerdyn Green (Gurit, Wattwill, Switzerland), further named KD, was taken for comparison.

2.2 | Reactive foam extrusion

Prior to the extrusion process, the PET was dried at 130°C for at least 24 h with a dew-point dryer (Gerco, Ennigerloh, Germany) in order to achieve residual moisture below 60 ppm. The residual moisture was determined with a Karl Fischer-Coulometer C30S with a Stromboli oven sample changer (Mettler Toledo, Columbus, OH). The foam extrusion was proceeded with a fixed throughput of 6 kg h⁻¹ of PET and 2% CO₂ on a Dr. Collin Tandem extrusion line (twin screw ZK 25 P, single screw E 45 M) (Dr. Collin GmbH, Maitenbeth, Germany), equipped with an oil heated slit die with opening

dimension of ($l \times b \times h$) 0.6 × 30 × 20 mm³. In order to achieve plate-like samples, the foam was conducted through a Dr. Collin Plate Calibrator with a gap height adjusted between 25 and 30 mm, while the width was varied between 130 and 150 mm, depending on the expansion force of the foam. The die and the melt temperature were adapted to the specific formulations in order to enable a stable extrusion process and can be found in Table 1. It has to be noted that the KD foam is produced differently (Breaker Plate and welding) compared to the own samples, which result in differences in morphology and homogeneity.

2.3 | Foam sample preparation

After calibration, the PET sheets exhibit significant foam skins. As the skin is compact and inhomogeneous, it has to be removed in order to obtain homogeneously foamed samples. This post-processing was proceeded with a Diadisc 6200 saw (Mutronic, Rieden am Forggensee, Germany).

Mechanical test specimen was cut with a geometry ($l \times b \times h$) of 10 × 10 × 10 mm³ for compression and 60 × 25 × 10 mm³ for three-point bending. Samples of 200 × 90 × 10 mm³ were prepared to perform single-flame source tests, 100 × 100 × 10 mm³ for cone calorimetry.

2.4 | Bulk sample preparation

Compounding was carried out using a co-rotating twin-screw extruder (Thermo Scientific Process 11 from Fisher Scientific, Waltham, MA) with a screw diameter of

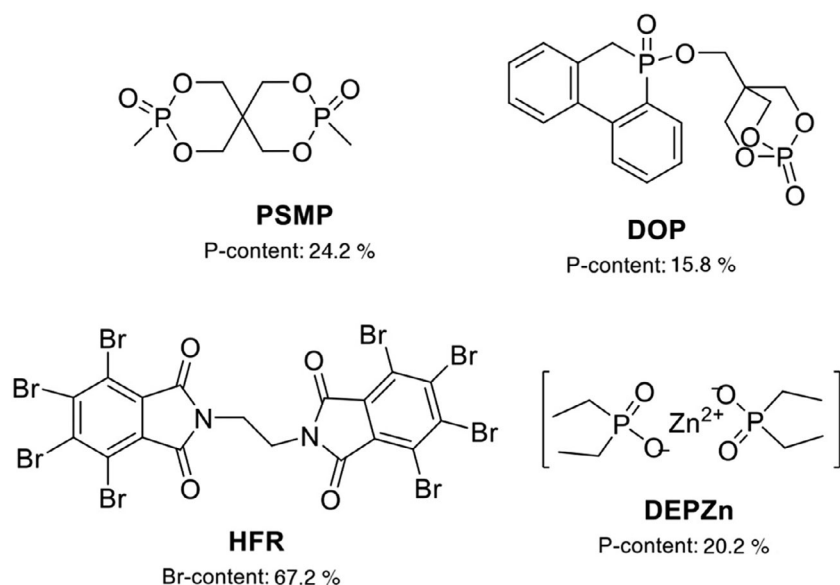


FIGURE 1 Flame retardants PSMP, DOP, HFR, and DEPZn

11 mm and a screw rotation speed of 150 rpm. The first temperature zone was set as 240°C, all other temperature zones were set to 270°C. The melt strand was cooled with a water bath and pelletized in a pelletizing system (Varicut, China, Shanghai, Jiading). The cone calorimeter samples were obtained by hot pressing (Dr. Collin GmbH) of the compounds at 270°C and 5 bar for 5 min.

2.5 | Characterization

2.5.1 | Gel permeation chromatography

To identify the effect of CE on the molecular weight of the PET foams, gel permeation chromatography (GPC) measurements of the different samples were conducted. The molecular weight (M_n and M_w) and polydispersity index (PDI) were determined by GPC. The GPC analysis was performed on a device having three PSS-PFG gel columns (particle size = 7 μm) with a porosity range from 100 to 300 \AA (PSS, Mainz, Germany) together with a Gynkotec refractive index detector (Dionex, Sunnyvale, CA). Hexafluoro-2-propanol (HFIP) (HPLC grade) with potassium trifluoroacetate (4.8 g in 600 mL HFIP) was used as eluent with a flow rate of 0.5 mL min^{-1} . As internal standard toluene (HPLC grade) was used. The calibration was done with narrowly distributed poly(methyl methacrylate) homopolymers (PSS calibration kit) that was used as a standard. The sample was dissolved in HFIP with potassium trifluoroacetate and filtered through a 0.22 μm PTFE filter before analysis. An injection volume of 20 μL was used for the analysis and the GPC columns were maintained at room temperature.

2.5.2 | Differential scanning calorimetry

Differential scanning calorimetry (DSC) was used to determine the crystallinity and the glass transition temperature. Therefore, a DSC1 Stare System (Mettler Toledo) was used. All the measurements were carried out in a temperature range of 25–300°C and a heating rate of 10 K min^{-1} with a nitrogen atmosphere (50 mL min^{-1}).

2.5.3 | Foam density

The density was measured according to the Archimedes principle. The measurements were performed in distilled water with an AG245 analytical balance (Mettler Toledo) with the use of a density kit for AG balances.

2.5.4 | Scanning electron microscopy

Scanning electron microscopy (SEM) analysis for investigations on the foam morphology was proceeded with a JSM-6510 (Jeol, Akishima, Tokyo, Japan). The cryogenic broken samples were sputtered with a 13 nm gold layer by using a Sputter Coater 108auto (Cressington, Watford, England). The gold used had 99.9% purity. For cell evaluation, the analytical program ImageJ 1.51m9 was used.

2.5.5 | FR testing

Cone calorimeter tests were conducted with an i-Cone Cone Calorimeter from Fire Testing Technology (East

Grinstead, United Kingdom) according to ISO 5660 with a heat flux of 35 kW m^{-2} and 25 mm gap size. All samples were tested in triplicate.

Single-flame source tests were performed according to EN ISO 11925-2.

2.5.6 | Mechanical properties

Mechanical testing was proceeded with a universal testing machine Zwick Z050 (Zwick/Roell, Ulm, Germany) equipped with a 50 kN load cell and corresponding compression or three-point bending tool. The compression modulus was determined according to DIN EN ISO 844 with a testing speed of 1 mm/min.

If the influence of the density on the compressive modulus is known,^[19] a normalization of the compressive strength σ_C and modulus E_C is possible. Due to the different effects of the FRs on the mechanical behavior, a direct relation between E_C and density of the foam related to a reference density by the use of a Gibson–Ashby Plot is not possible with the given sample matrix.^[20–22] Lobos and Velankar investigated different methods for the normalization of mechanical data at different foam densities combined with Nano fillers.^[23] In conclusion, any relation between mechanical values and density has to be seen with caution, whereas the use of a Gibson–Ashby Plot is the most promising approach. If this is not possible, any other relationship allows us to draw at least a better comparison than ignoring the density difference completely. With regards to the given material information and result basis of the own materials, only a specific compressive strength at 10% deformation $\sigma_{Cs\ 10\%}$ and modulus E_{Cs} can be determined, according to the following equations:

$$E_{Cs} = \frac{E_{\text{foam}}}{\rho_{\text{foam}}} \quad (1)$$

$$\sigma_{Cs\ 10\%} = \frac{\sigma_{10\%\text{foam}}}{\rho_{\text{foam}}} \quad (2)$$

The drawback of this method is that a linear relationship between mechanical properties and foam density is expected, which is seen crucial especially at high densities.^[23] Nonetheless, the resulting values provide a better comparability than without normalization.

The three-point bending modulus E_B and strength σ_B were determined according to DIN 53423, adapted to the specimen geometry with 10 mm min^{-1} speed and 50 mm effective span. The values were also normalized according to Equations (1) and (2).

3 | RESULTS AND DISCUSSION

3.1 | Reactive foam extrusion

With the optimized parameters and mixtures listed in Table 1, a stable and reproducible processing of the different PET foams without calibration was possible. The CE content was adapted to maintain the process stability, whereas the expansion ratio and foam morphology were tried to keep comparable. The FR content was chosen as low as possible to maintain a stable foam extrusion process. With 5 wt% of PSMP, no foam was obtained so the FR content was modified to the foam extrusion process. In the case of PSMP, the foams with 3 wt% were hardly comparable to the others with regards to process stability. Thus, trials revealed 2 wt% PSMP combined with ZnSt were suitable for a stable foaming process. Foam samples containing DOP were only possible with concentrations of 3 wt% to obtain comparable foam morphologies. However, the subsequent calibration step has an influence on the resulting foam morphology and density. The processing parameters and density values are summarized in Table 1, the detailed results of the DSC measurements can be found in the Table S1.

Due to the calibration process after foam extrusion, a piling of the foam takes place, which enables the formation of air pockets that are larger than the foam cells (Figure S1). This and the tribology of the hot extrudate passing through the calibrator lead to several challenges with regard to the adjustment of the final density. The balance between density, proper plate geometry, and processability was optimized for each foam system separately. Although a close density range of all foams is achieved with the slit die, around 100 g L^{-1} (density sd.), the subsequent calibration process resulted in a significant drift of the density in a range of 157 and 401 g L^{-1} (density cal.) among the different samples. The density and morphology are more comparable to the reference system KD after calibration. The pressure at the die (p_D) is important for foaming, as it defines the pressure drop rate and thus the nucleation and formation of the cells. A p_D around 100 bar was found to be most suitable for a stable and reproducible process. However, not all materials were suitable for the foam extrusion at these conditions as seen with 3 wt% PSMP and 2 wt% DOP. It is well known that due to the semicrystalline structure of PET, a narrow processing window is given where slight changes in T_D and T_M are notably affecting the foaming behavior.^[24–26] The main reasons for adaptations during processing are the different FR additives, which also required an adaption of the CE content. High amounts of PSMP and DOP affected the melt viscosity significantly during extrusion, either by an increased degradation

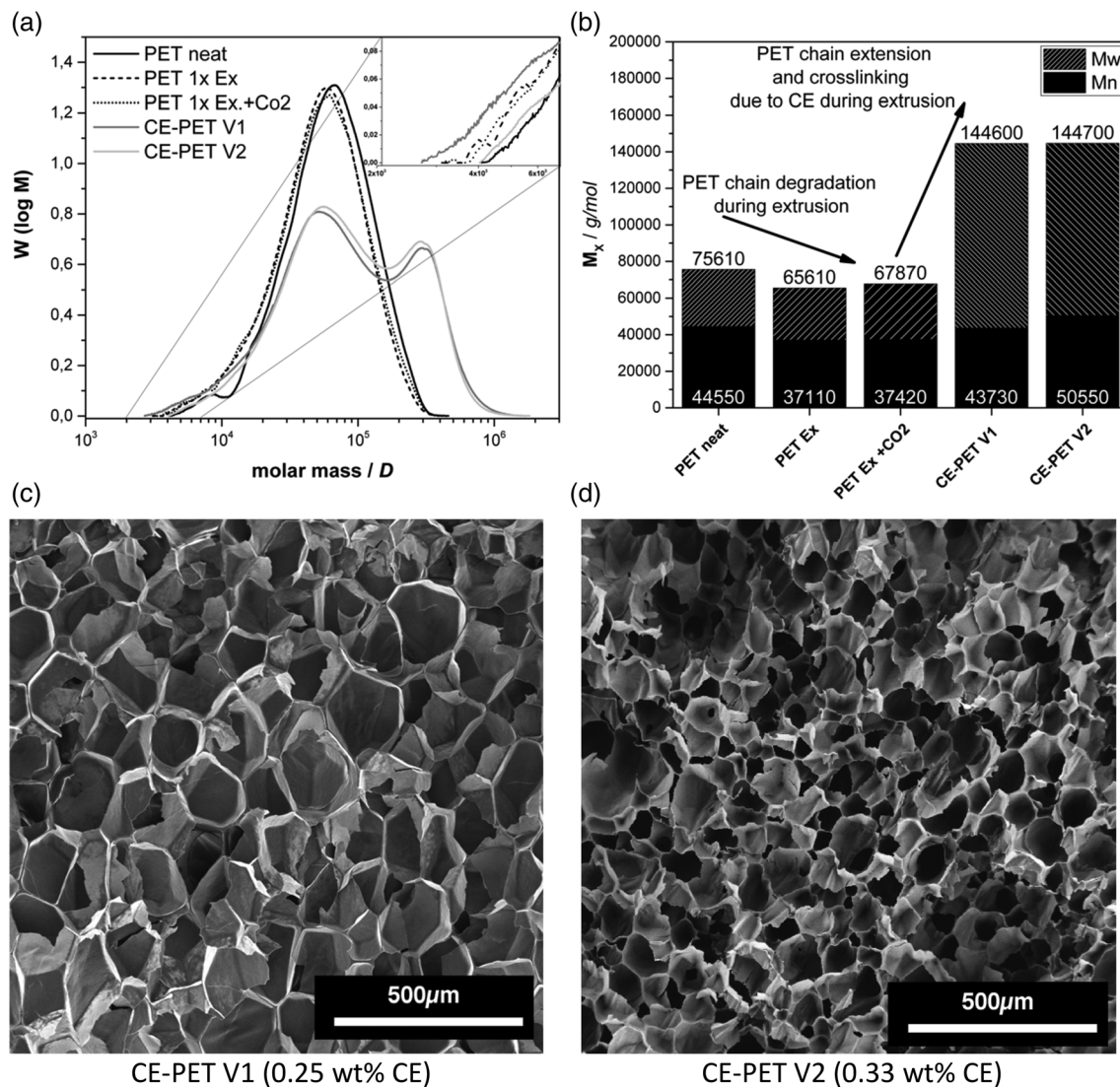


FIGURE 2 (a) Molar mass distribution as received from GPC for different PET samples with detailed region around 2,000–7,000 D. (b) Change of molecular weight of PET at different processing steps. While PET neat, PET Ex, and PET Ex + CO₂ contain no CE, CE-PET V1 contains 0.25 wt% and CE-PET V2 0.33 wt% PMDA. (c) Foam morphology of CE-PET V1. (d) Foam morphology of CE-PET V2

(Figure 2b) or by an additional lowering of viscosity. As a result, the FR content was lowered and/or the CE content increased in order to gain a sufficient p_D .

3.2 | Foam properties

3.2.1 | Thermal properties

Regarding the glass transition temperature (T_g), all samples are in a close range to neat PET with $80 \pm 2^\circ\text{C}$ independent from CE and FR content. The melt temperature (T_m) of PET prior to the extrusion process with 249°C is lowered down to the range of $240\text{--}243^\circ\text{C}$ when the material was processed with CE and different FRs. This decrease in T_m due to chain extension

combined with a decrease in the crystallization enthalpy is already described in literature. It is explained by changes in the molecular structure of the PET chains due to the CE, affecting the crystallinity due to branching. This complicates the ability of the polymer chain to assemble into a crystal lattice.^[27–29] In addition, the crystallinity, as indicated by the crystallization enthalpy, is expected to be lowered with increasing the molecular weight due to branching and crosslinking.^[27,30] The effective influence on the degree of crystallinity (X_c) of the PET samples was calculated by the following equation:

$$X_c = \frac{\Delta H}{\Delta H_0} \times 100\% \quad (3)$$

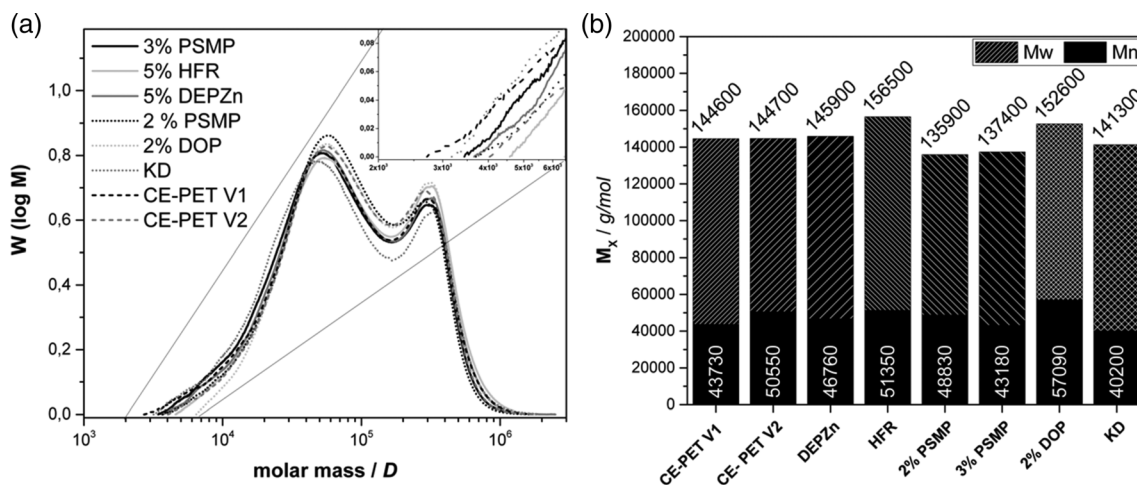


FIGURE 3 (a) Molar mass distribution as received from GPC for PET + CE + FR samples with detailed region around 2,000–6,500 D. (b) Molecular weight (M_n black and M_w shaded) of PET foams with CE and different FR additives

where ΔH is the melting enthalpy of the samples and ΔH_0 the enthalpy of melting for a 100% crystalline PET sample, which is indicated as 140 J g^{-1} in literature.^[27,31]

In most cases, this can be confirmed as the degree of crystallinity with 22.86% of the unfoamed and non-chain extended PET is lowered between 0.72%, to a value of 22.14% at CE-PET V2 and 2% DOP samples, and 3.57% to a value of 19.29% at the 5% DEPZn sample.

However, an increased crystallinity of 24.29% can be observed at 2 wt% PSMP. This can be contributed to the chain degradation, as this sample exhibits the lowest molecular weight, see later discussion (Figure 3b). The added highly crystalline ZnSt in 2 wt% PSMP sample, with a total of 0.1 wt%, might also cause nucleation spots for crystallization of PET and thus increase the crystallinity. Detailed values can be found in Table S1.

3.2.2 | Morphology and molecular weight

Due to the influence of the FRs on the extrusion process, the CE content was adjusted in a range between 0.25 and 0.5 wt%, whereas the lowest content was aimed for each mixture. Figure 2 illustrates the change in the molecular weight of the PET without FR caused by different processing steps and CE contents, as well as the influence of the CE content on foam morphology. The *PET neat* sample corresponds to the PET granule from stock without any processing, while *PET Ex* means the PET granule is extruded once at processing conditions without any CE modification, *PET Ex + CO₂* corresponds to the same processing conditions with additional CO₂ loading (2%) according to the later foams. CE-PET V1 and CE-PET V2

correspond to the different foaming systems, where CE is added by 0.25 and 0.33 wt%, respectively.

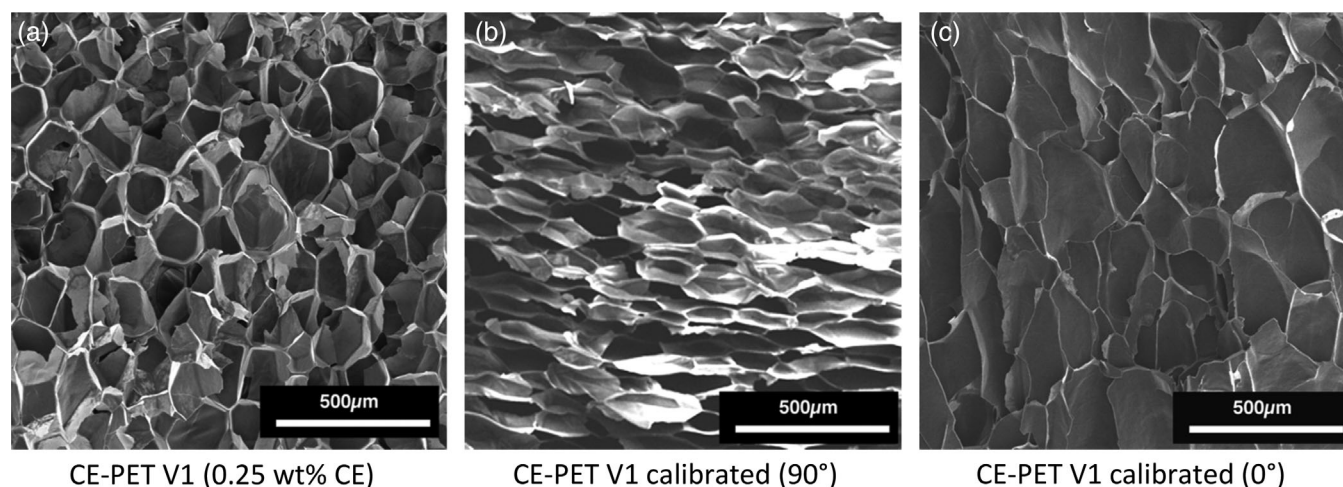
It is observed from Figure 2a and Figure 2b that the extrusion process leads to a chain degradation when no CE is added. This can be explained by high shear during extrusion, as well as residual moisture and moisture uptake in the hopper. When CO₂ is added, the shearing is lowered due to the plasticizing effect, leading to slightly increased M_w and M_n . However, the sample PET Ex + CO₂ is not able to foam properly. A degradation effect with CE can still be observed in Figure 2a, where CE-PET samples also show lower molecular weights compared to the unprocessed PET neat. However, the addition of 0.25 wt% CE at CE-PET V1 results in a bimodal molecular weight distribution and an overall peak broadening up to higher molecular weights. The M_n increases close to its value prior to the extrusion process, while the M_w is more than doubled and the PDI increases from 1.70 to 3.31. This indicates that the CE counteracts the general chain degradation during the processing, leading to the observed chain growth and branching, which is resulting in a proper foamability at the same extrusion conditions. Thus, 0.25 wt% was chosen as a minimum CE content for this study. It confirms the expectation that low IV PET can be foamed properly with the addition of CE only, as the molecular weight has to be increased for sufficient melt strength. As PMDA is a four-functionality CE, it also leads to chain branching, which is even more favorable for foaming.^[9–11] The higher CE content of 0.33 wt% increases especially the M_n value at CE-PET V2, while M_w remains nearly constant. This can be explained by a decreased number of small molecules that can react with the additional CE. This is confirmed by the GPC curves (Figure 2a) and indicated by PDI (Table 1), as it is decreasing from 3.31

TABLE 2 Overview of the cell size and cell densities achieved with different PET foam samples prior to the foam calibration process

Sample	CE (wt%)	Foam density sd. (g L ⁻¹)	Average cell size (μm)	Cell density (cells mm ³⁻¹)
CE-PET V1	0.25	105 ± 5	185 ± 62	4.44 × 10 ⁵
CE-PET V2	0.33	89 ± 1	101 ± 36	3.10 × 10 ⁶
5 wt% DEPZn	0.35	105 ± 2	193 ± 65	3.79 × 10 ⁵
5 wt% HFR	0.25	95 ± 2	84 ± 32	6.30 × 10 ⁶
3 wt% PSMP	0.35	132 ± 10	153 ± 66	8.97 × 10 ⁵
2 wt% PSMP ^a	0.40	93 ± 4	94 ± 40	2.36 × 10 ⁶
2 wt% DOP	0.35	91 ± 4	94 ± 40	4.21 × 10 ⁶
KD ^b	–	190 ± 15	292 ± 176	8.27 × 10 ⁴

^aContains ZnSt in a 20:1 ratio PSMP:ZnSt.

^bCalibrated, evaluated in homogeneous region.

**FIGURE 4** SEM images of CE-PET v1 (a) uncalibrated, (b) calibrated, view in 90° to extrusion and (c) calibrated, view in extrusion direction (0°)

to 2.86 and designating a more uniform molecular weight distribution. This is also reflected in differences in the foam morphology as observed in Figure 2c and 2d. The detailed numbers are found in Table 2.

The molecular weight distribution is affected by the added FRs with different effects leading to an increased or decreased M_w , M_n , and PDI. Figure 3 illustrates the change in the molecular weight of the PET with FR and adapted CE contents.

It can be observed that all foams exhibit a bimodal distribution (Figure 3), as well as an M_n between 40,000 and 57,000 g mol⁻¹ and an M_w between 135,000 and 156,500 g mol⁻¹. 2 wt% DOP has less influence compared to the others, resulting in the highest M_n and M_w combined with the lowest PDI. At 5-wt% DEPZn, the M_w and M_n remain between CE-PET V1 and CE-PET V2. This indicates a higher amount of small chains remaining, also 0.02 wt% more CE is added compared to CE-PET V2. Thus, a certain chain degradation effect can be contributed to 5 wt% DEPZn. For both PSMP

samples, a drop around 10,000 g mol⁻¹ in M_w can be observed, although a relatively high amount of CE was added. As already seen at the CE-PET samples, the higher amount of CE at 2 wt% PSMP leads to an increase of M_n , which means that the branching process of the CE counteracts the chain degradation of the added PSMP. Nonetheless, the average chain length is significantly decreased. This can be contributed to the known chain degradation caused by PSMP. The added amount of ZnSt is noted to show a slight influence on the molecular weight. As 5-wt% HFR contains 0.25 wt % CE only, this additive exhibits the lowest influence on PET chains as M_w and M_n are increased even further compared to CE-PET V1 with the same amount of CE but no FR inside and even CE-PET V2 with 0.1 wt % more CE. As a reason, the strong hydrophobic and inert nature of 5 wt% HFR can be seen, which reduces the overall residual moisture content and excludes any interaction with PET, being beneficial with regards to chain degradation.

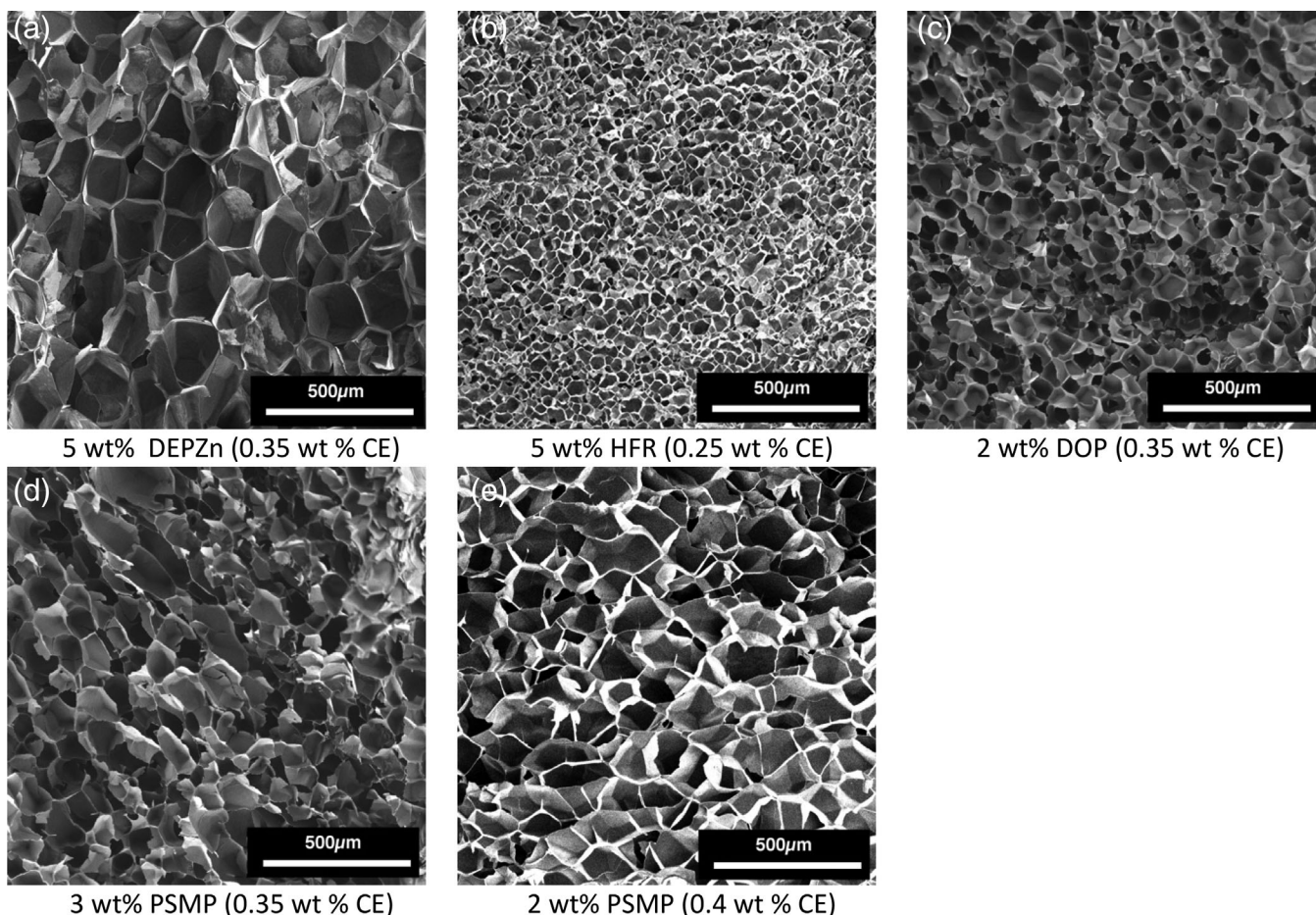


FIGURE 5 SEM images of foam morphology of the five different flame retarded foams (a to e) before calibration as used for cell evaluation taken in 0° orientation

A comparison between calibrated and uncalibrated foams is presented in Figure 4. The calibration process leads to a distortion of the cells in the calibration direction.

As the squeezed cells after calibration (Figure 4b and 4c) are not suitable for cell evaluation due to undefined lateral deformations in 0 and 90° orientation to the extrusion direction, uncalibrated samples were chosen for evaluation. The morphology of the different flame-retarded foams before calibration is shown in Figure 5.

A nearly homogeneous foam morphology can be confirmed for all foams. However, an expected difference in cell size and cell density can be observed among the samples as summarized in Table 2. As the CO_2 content was constant among all samples, the differences result mainly from the type of FR and the correlated CE content. The adapted process temperatures are supposed to play a secondary role regarding the morphology formation.

The higher CE content and the resulting increased melt strength of CE-PET V2 lead to a smaller cell size and higher cell density. The 5 wt% HFR is expected to

remain as solid, as its melting temperature with around $465^\circ\text{C}^{[32]}$ is beyond the processing temperature (T_{max} in barrel 275°C). Thus, it is expected to remain as fine dispersed inert filler particles, which act as a nucleating agent for foam cell formation. This is confirmed by the smallest cell size and highest cell density among all samples. PSMP (T_m around $245^\circ\text{C}^{[33]}$) is close to its melt temperature. Thus, it freezes in the same range as the matrix PET. This can affect the cell formation directly and also lead to a certain cell nucleation by the formation of first crystals. Nevertheless, the lowered molecular weights for samples containing PSMP affect the cell stability and growth more significant, leading to smaller cells at 2 wt% PSMP compared to 3 wt% PSMP. 2 wt% DOP (T_m around $234^\circ\text{C}^{[34]}$) and 5 wt% DEPZn (T_m around $200^\circ\text{C}^{[35]}$) are expected to be completely molten at the given extrusion conditions. Thus, both fillers cannot act as nucleating agents and freeze in the PET matrix. In this case, the melt strength is the guiding factor for cell growth when comparing CE-PET V1, 5 wt% DEPZn, and 2 wt% DOP. While CE-PET V1 and 5 wt% DEPZn own a narrow cell size and molecular weight distribution, the increased

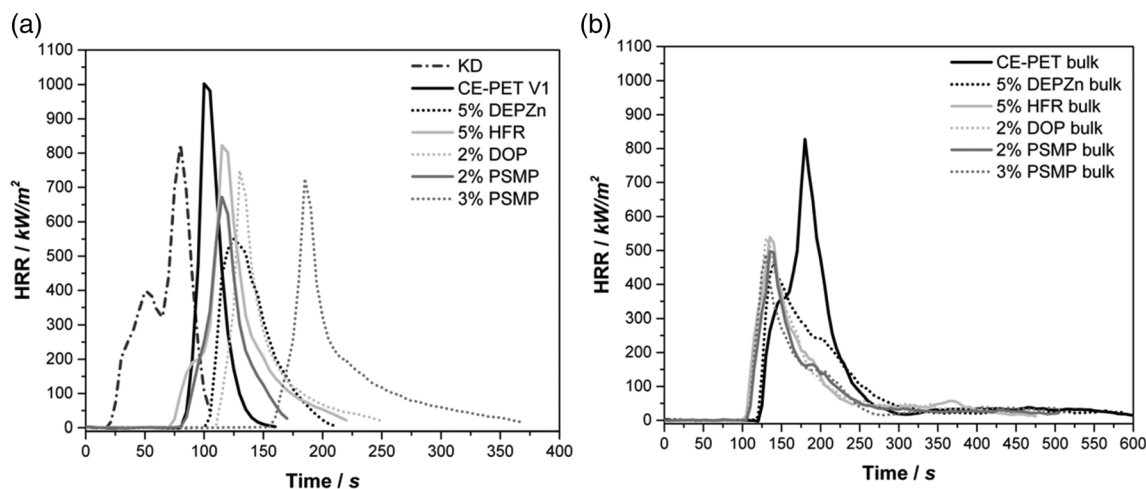


FIGURE 6 Heat release rate (HRR) curves over time with an irradiation of 35 kW m^{-2} and 25 mm gap. (a) Foams with a sample size of $100 \times 100 \times 10 \text{ mm}^3$ (b) Bulk samples with a size of $100 \times 100 \times 2 \text{ mm}^3$

molecular weight of 2 wt% DOP is resulting in notably smaller cells. However, an influence of the melt and die temperature during the extrusion process cannot be excluded as 2 wt% DOP had to be processed at a T_D 10°C lower compared to CE-PET and 5 wt% DEPZn, while the T_M was in a close range. The average cell size is in accordance with the foam density prior to the foam calibration process. Samples containing 5 wt% HFR and 2 wt% DOP possess the lowest cell size whereas samples containing 5 wt% DEPZn, 3 wt% PSMP, and CE-PET V1 exhibit the largest cell sizes. This leads to the assumption that small cell sizes can be achieved by nucleating effects (HFR) and/or a high M_n (DOP, CE-PET V2) under the given foaming conditions.

In summary, the reactive foam extrusion process of PET with PMDA in presence of different FRs is leading to comparable molecular weights and its distribution, as well as smaller and closer distributed cell sizes compared to the reference foam core material KD. The type of FR is significantly influencing the processing behavior of the systems.

3.3 | FR properties

Cone calorimetry tests were performed for the different PET foamed and unfoamed samples. The heat release rate (HRR) is shown in Figure 6, the numerical values are summarized in Tables 3 and 4.

The heat release over time and total heat release (THR) development of the foamed samples are shown in Figure S2a, while the development of smoke release is shown in Figure S2b.

Due to the maintenance of the process stability, the foam samples show a wide spread of sample weight,

which differs between 16 and 39 g depending on the density. In contrast, the bulk samples have similar sample weights of 33 g. Due to the larger surface to volume ratio for the foam samples, the surface is more accessible for heat sources in comparison to bulk samples, which leads to shorter burning times even if there is a higher amount of combustible material in the foam samples than for the corresponding bulk samples. The initial sample weight of 3 wt% PSMP is 5 g higher than the corresponding bulk sample and the burning time is almost doubled for the bulk sample. Due to the requirement of plane samples for cone calorimetry measurements, the foam densities of the calibrated foams have to be considered for the interpretation of the results. It is known that the density influences the HRR, as the amount of combustible material is dependent on the density. 3 wt% PSMP is the densest material (401 g L^{-1}) of all foam samples and has a long burning time. CE-PET V1 presents lowest density (157 g L^{-1}), while 5 wt% HFR and 2 wt% DOP have similar densities ($245\text{--}253 \text{ g L}^{-1}$) but only the flame-retarded samples have a similar burning times (151–155 s) whereas the neat PET foam has a very short burning time (–50%). The addition of phosphorus-containing FRs into the PET foams leads to a longer burning time with equal and unequal densities of the foams.

The PET foam containing 5 wt% HFR has the shortest time to ignition (TTI) with 76 s whereas neat PET foam ignites after 83 s. The addition of different phosphorus-containing FRs results in a TTI of 90 (5 wt% DEPZn) up to 163 s (3 wt% PSMP). 3 wt% PSMP has the longest TTI with 163 s whereas 2 wt% PSMP results in a TTI of 95 s. The peak heat release rate (PHRR) can be reduced by up to 31% by the addition of 2 wt% PSMP. The lowest PHRR reduction is caused by 5 wt% HFR with 15%, the other flame-retarded samples achieve a reduction of about

TABLE 3 Cone calorimetry results (25 mm gap, irradiation 35 kW m⁻²) of the PET foams (100 × 100 × 10 mm³)

Sample	TTI (s)	PHRR (kW m ⁻²)	PHRR reduction (%)	THR (MJ m ⁻²)	MARHE (kW m ⁻²)	TSR (m ² m ⁻²)	Foam density cal. (g L ⁻¹)
CE-PET V1	83	947.12	–	22.94	169.39	510.60	157 ± 8
5 wt% DEPZn	90	696.30	28.56	20.65	140.18	777.30	193 ± 8
5 wt% HFR	76	822.09	15.66	32.62	178.03	1,066.41	253 ± 24
3 wt% PSMP	163	725.03	25.61	30.60	96.61	745.12	401 ± 78
2 wt% PSMP ^a	95	669.26	31.34	22.35	131.79	498.79	221 ± 16
2 wt% DOP	112	748.82	23.17	24.26	113.68	433.23	245 ± 16

^aContains ZnSt in a 20:1 ratio PSMP:ZnSt.

TABLE 4 Cone calorimetry test results (25 mm gap, irradiation 35 kW m⁻²) of bulk PET samples (100 × 100 × 2 mm³)

Sample	TTI (s)	PHRR (kW m ⁻²)	PHRR reduction (%)	THR (MJ m ⁻²)	MARHE (kW m ⁻²)	TSR (m ² m ⁻²)
CE-PET V1	119	699.17	–	50.49	171.86	1,135.66
5 wt% DEPZn	122	461.94	39.47	43.97	135.86	1,390.30
5 wt% HFR	108	539.18	29.34	38.87	136.39	1,309.95
3 wt% PSMP	110	488.13	36.03	34.58	114.19	1,270.71
2 wt% PSMP ^a	110	419.36	45.04	31.48	118.25	1,247.54
2 wt% DOP	105	535.30	29.85	38.33	134.53	976.35

^aContains ZnSt in a 20:1 ratio PSMP:ZnSt.

23–31%. The THR is reduced only by the addition of 2 wt% PSMP and 5 wt% DEPZn. The total smoke release (TSR) is significantly increased for the halogen-containing sample 5 wt% HFR with 1,066 m² m⁻².

A reduction in TSR can be observed for 2 wt% DOP and 2 wt% PSMP whereas 3 wt% PSMP has the highest TSR indicating a gas phase activity. In summary, the samples consisting of phosphorus-containing flame-retarded foams showed the best fire behavior regarding cone calorimetry tests in terms of PHRR, TSR, and THR. PSMP consists of a phosphonate moiety whereas DOP combines a phosphonate and a phosphate moiety with lower total phosphorus content of 8% than PSMP. 2 wt% DOP and 3 wt% PSMP contain the same amount of CE and can be distinguished by the TTI, which is 51 s longer for 2 wt% DOP. However, the TSR of 3 wt% PSMP is 311 m² m⁻² higher than that of 2 wt% DOP. It has to be considered that PSMP shows a gas phase activity in PET whereas the phosphate moiety remains mainly in the condensed phase.^[18,36] The foam 3 wt% PSMP contains 0.35 wt% CE. The addition of ZnSt to 2 wt% PSMP for a reduction of chain degradation leads to an increased consumption of CE (0.4 wt% CE) generating a stable foam extrusion process. In addition, ZnSt is known as a

nucleating agent in polymer foams.^[37] Comparing 2 wt% PSMP and 3 wt% PSMP, the PHRR is lowered from 725 (3 wt% PSMP) to 669 kW m⁻² (2 wt% PSMP) and the TSR is lowered from 745 (3 wt% PSMP) to 498 m² m⁻² (2 wt% PSMP). DEPZn and PSMP are known to be mainly active in the gas phase.^[18,36,38] At similar calculated total phosphorus content in the foam, 2 wt% PSMP and 5 wt% DEPZn show similar PHRR and THR results. In sum, 2 wt% PSMP has the best fire performance in combination with a stable foam extrusion process. The PHRR is lowered by 31% and the foam density is in a similar range of the neat PET foam. The overall performance of 5 wt% DEPZn is slightly decreased than 2 wt% PSMP. 2 wt% DOP and 5 wt% HFR also show adequate foam densities but the fire behavior regarding the PHRR reduction is 16–23%.

Regarding the bulk PET samples, it becomes obvious that the samples containing FRs show no significant difference in the cone calorimetry results as for the foamed samples. The flame-retarded bulk samples show a PHRR of 419–539 kW m⁻² whereas the flame-retarded foamed samples show a PHRR of 669–822 kW m⁻². It is obvious that the fire behavior regarding the PHRR reduction is better for 2 wt% PSMP (45%) than for the sample

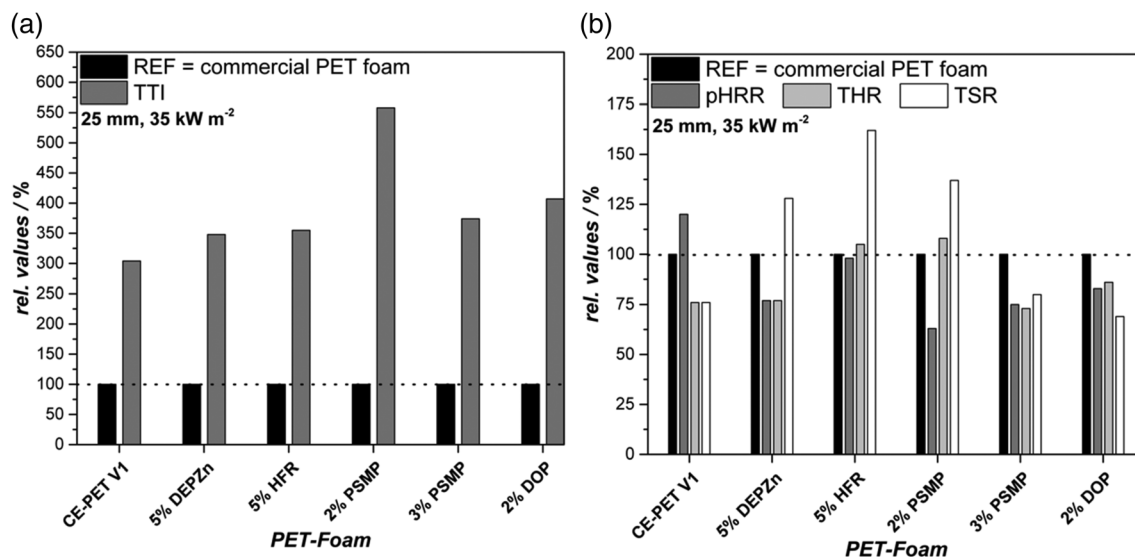


FIGURE 7 Relative comparison between PET cores containing no flame retardant (CE-PET), 5% DEPZn and 5% HFR, 2% and 3% PSMP and 2% DOP as flame retardant with commercial KD foam (=100% black bar for all values) at 35 kW m^{-2} heat flux and 25 mm gap. (a) TTI values, a TTI above 100% is beneficial compared to the reference; (b) Comparison of relative pHRR, THR, and TSR values below 100% indicates a better performance compared to the reference

containing 3 wt% PSMP (36%). The sample containing 2 wt% PSMP also contains zinc stearate, which enhances the processability during the extrusion process (foam and bulk). A higher amount of PSMP leads to an increased chain degradation.

In general, it is observed that the flame-retarded bulk samples show a similar burning behavior among each other, while the flame-retarded foam samples do not. This can be seen by different HRR curve characteristics during cone calorimetry (Figure 6).

This leads to the assumption that foamed PET requires less amount of FRs than corresponding bulk samples for a quantifiable FR efficiency, which is also dependent on the resulting foam density. The foam density is a function of the processability, which can be adjusted by the amount of CE. In compliance with ISO 5660^[39] the foam samples are thick samples and the bulk samples are thin samples. The foams are thermally thinner than the corresponding bulk samples due to the insulation properties of foams going along with a larger PHRR, which is in accordance with the literature.^[40]

Figure 7 compares the performance of the different flame-retarded PET cores, whereas the commercial foam KD was chosen as a 100% relative value. In the case of TTI, values above 100% are favorable as there is more time until ignition. In the case of PHRR, THR, and TSR, values below 100% are beneficial, as lower values compared to the reference are desired.

The TTI is notably increased among all samples when compared to KD. As the thermal conductivity plays a key role for TTI, some fillers in the KD sample are expected

to increase its thermal conductivity leading to faster ignition. This aspect was not investigated further, as it is not in the scope of this research. Samples containing 3 wt% PSMP and 2 wt% DOP show better results for all values. The sample containing 5 wt% HFR performs better in the case of TTI, while PHRR is nearly the same, the THR is 8% increased and the TSR even 37% compared to KD.

In contrast to the cone calorimetry testing, the single flame testing shows no significant difference in the burning behavior among the foam samples. All of them show self-extinguishing behavior and reached an *E* classification, as a dipping without burning was observed. The details of the results are summarized in Table S2.

3.4 | Mechanics

The resulting anisotropic cell orientation due to the calibration is leading to a dependence of the mechanical properties on the load direction. As the sample geometry is limited, only compression tests were carried out in horizontal 0° (in extrusion direction) and vertical 90° (vertical to extrusion direction) load direction while three-point bending tests were performed in 90° orientation only. An exemplary plot of the different characteristic curves can be found in Figure 8.

As observed from Figure 8, the compressive modulus and strength are increased in a 90° load direction. This can be explained by the orientation and compaction of the foam cells. The amount of load-bearing cell struts is

increased by 90° orientation, leading to higher stress required for cracking which is kept during the whole testing. In contrast, the 0° sample has a higher number of small struts for load-bearing only, leading to a continuous increase of stress during testing. The specific normalized compression and bending modulus, (E_{Cs}) and (E_{Bs}), as well as the specific normalized compressive stress at 10% strain ($\sigma_{Cs,10\%}$), and maximum stress before brake at three-point bending (σ_{Bs}) are compared in Figures 9 and 10. The normalization was proceeded according to Formulas (1) and (2). The numerical values of the measured and normalized values can be found in the Supporting Information.

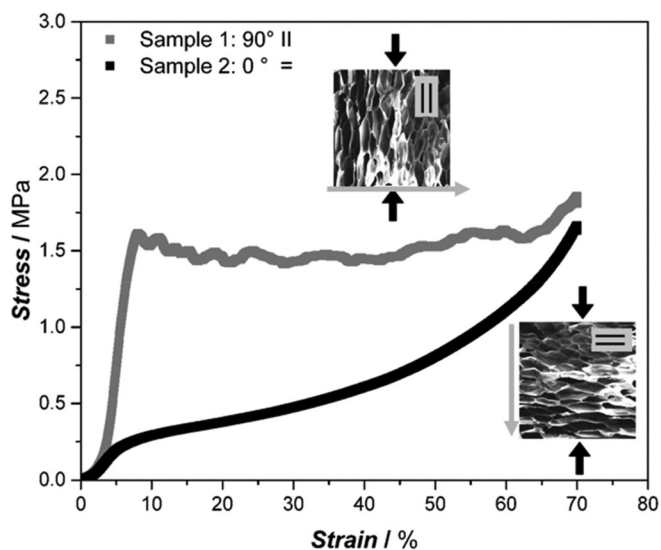


FIGURE 8 Typical compression curves received from 0° (in extrusion direction) and 90° (vertical to extrusion direction) loading, examples taken from 5% DEPZn samples. The extrusion direction is indicated by gray arrows next to the SEM morphology indicators

The compression load direction effect as shown in Figure 8 is confirmed for all samples. As the normalization of the values by the foam density was proceeded, a better comparison of the samples can be drawn. Numerical values of the compression test results, also uncorrected, can be found in Table S3, for three-point bending Table S4. In general, the addition of FR increases the mechanical performance in bending and compression. The samples with smaller cell sizes and higher molecular weight, namely 5% HFR, 2% DOP, and 2% PSMP, show the highest compression performance. The bending performance is also notably influenced by the type of filler and resulting morphology. Also, the 2% DOP sample provides fine cell morphology, a low bending modulus and strength are observed, while 5% HFR and 2% PSMP provide high strength and density values. This

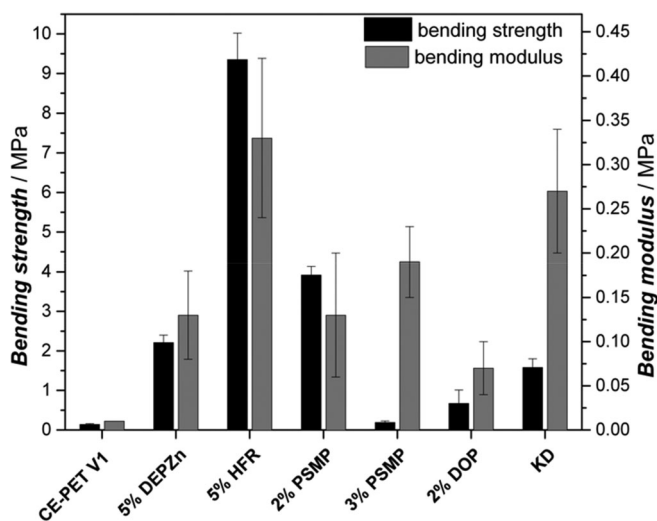


FIGURE 10 Normalized bending modulus (E_{Bs}) and stress at break (σ_{Bs}) of 90° samples

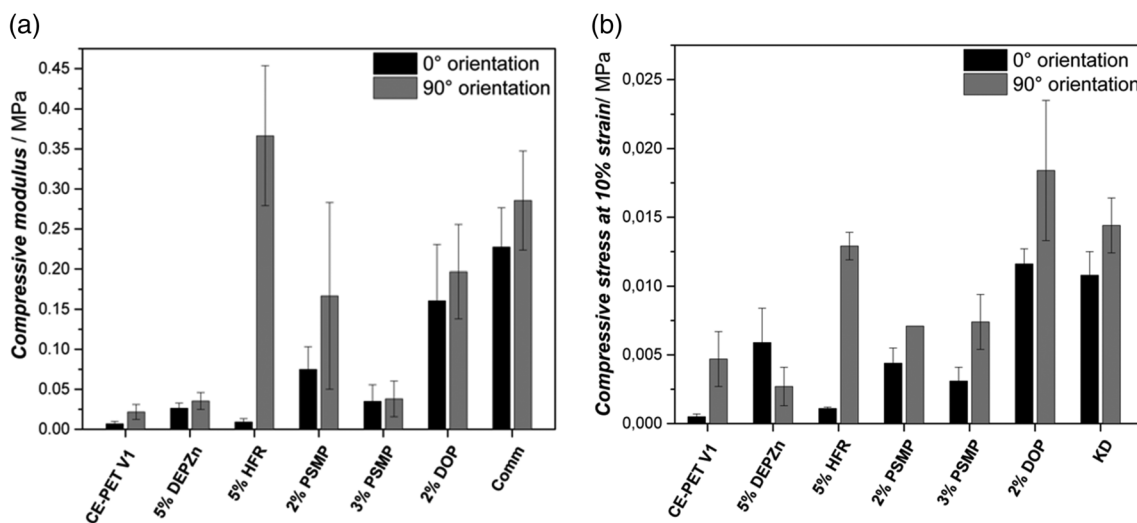


FIGURE 9 (a) Normalized compressive modulus (E_{Cs}) and (b) normalized compressive strain ($\sigma_{Cs,10\%}$) results of 0° and 90° samples

can be explained by a weak reinforcing effect of the 2% DOP containing sample in the struts. The notable chain degradation at 3% PSMP results in a weak bending performance comparable to the CE-PET samples, also a reinforcing effect of PSMP is shown in the sample containing 2% PSMP. An effect of the CE can be expected in this case, as the 2% PSMP sample contains the highest CE content. However, the molecular weight is lower compared to 2% DOP. The high performance of the 5% HFR sample can be contributed to the high molecular weight of the samples, which provides combined with the filler a proper reinforcement. As no direct information about the crosslinking is given, an influence regarding this aspect cannot be excluded completely. The processing method and post-processing of the commercial foam allow more homogeneous cell size and orientation. Nonetheless, a dependence on load direction was also found in compression testing.

4 | CONCLUSION

A bottle-grade PET was successfully foamed by reactive foam extrusion, using PMDA as a chemical modifier, in the presence of different FRs. As FRs, different commercially available types, containing halogen (HFR), phosphate (DOP), phosphinate (DEPZn), and phosphonates (DOP, PSMP) were used and compared. The molecular weights, thermal properties, the average cell size, and density of all foamed samples were determined by GPC, SEM, and DSC. The extrusion behavior was found to be significantly influenced by the different types of FR. This was limiting the amount of FR in the foam samples. 3% PSMP was found to be less suitable for PET processing, as a significant chain degradation of the PET matrix and processing fluctuations could be observed. Lowered amounts of 2 wt% PSMP combined with the processing additive ZnSt and an increased amount of CE resulted finally in proper foams with adequate process stability and a significantly improved FST behavior. 5% DEPZn and 2% DOP lead to homogeneous foams with small cell sizes and adequate processing. While the single flame test revealed a similar behavior among all samples, the cone calorimetry revealed notable differences among the samples. 5% HFR resulted in the most stable processing and finest cell sizes, but the TTI is shorter than neat PET whereas all other flame-retarded foams have significantly higher TTIs. Small amounts of different FRs in the PET foams are suitable for a PHRR reduction of up to 31% in the case of 2 wt% PSMP whereas the corresponding bulk samples show no significant reduction in PHRR. The normalization of mechanical values to its related foam density was used in order to provide a basic comparison;

also, it is known that several assumptions have to be taken. In general, an improvement of modulus and strength in compression and three-point bending testing can be observed when FRs are added to the CE-PET system. The calibration step after extrusion leads to an orientation of the foam cells, leading to better compressive values in the 90° load compared to the 0° orientation. This effect is used in commercial systems by special post-processing steps in order to design mechanical properties in desired orientations of the later foam sheets. The three-point bending test in 90° orientation revealed a higher bending strength of 5% DEPZn, 5% HFR, and 2% PSMP compared to the KD reference, while only 5% HFR reveals a higher modulus. The compression testing in 90° orientation revealed a higher compressive strength of 2% DOP and a close value of the 5% HFR sample compared to KD, while the modulus is higher only at 5% HFR. As expected, the testing in 0° orientation revealed a different behavior among all samples. In this direction, only the compressive strength of 2% DOP is slightly higher compared to KD, while the modulus is lower compared to KD among all samples. Thus, HFR and DOP can be seen as the most beneficial additives with regards to the mechanical properties. It is expected that KD include multiple additives that also support the mechanical properties. Thus, further improvement of the other systems can be expected by the addition of additional fillers, such as talcum or clays.

In conclusion, the upcycling of bottle-grade PET by chemical modification in the presence of FRs shows a high potential for the production of high-performance sandwich core materials.

ACKNOWLEDGMENTS

The authors would like to thank the German Research Foundation (DFG) for financial support (Project Number 278300368: AL 474/28-1 and DO 453/9-1). Furthermore, we would like to thank the Department of Macromolecular Chemistry II at the University of Bayreuth for the opportunity to measure GPC, Prof. Dr. Josef Brey and Florian Puchtler of the Department of Inorganic Chemistry II at the University of Bayreuth for the ability and assistance to proceed the cone measurements, and the Bavarian Polymer Institute (BPI) for the ability to work in their labs and equipment.

ORCID

Volker Altstädt  <https://orcid.org/0000-0003-0312-6226>

REFERENCES

- [1] L. Sorrentino, E. Di Maio, *J. Appl. Polym. Sci.* **2010**, *116*, 27.
- [2] S. T. Lee, N. S. Ramesh, *Polymeric Foams: Mechanisms and Materials*, CRC Press LLC, Boca Raton, FL **2004**.

- [3] R. Gendron, *Thermoplastic Foam Processing: Principles and Development*, CRC Press LLC, Boca Raton, FL **2005**, p. 67.
- [4] Z. Yang, C. Xin, *Adv Polym Technol.* **2018**, *37*, 2344.
- [5] T. Standau, B. Hädel, *Ind. Eng. Chem. Res.* **2018**, *57*, 17170.
- [6] T. Standau, C. Zhao, *Polymers* **2019**, *11*, 306.
- [7] T. Standau, S. M. Castellón, *e-Polymers* **2019**, *19*, 297.
- [8] F. Awaja, F. Daver, *J. Therm. Anal. Calorim.* **2004**, *78*, 865.
- [9] S. Japon, L. Boogh, *Polymer* **2000**, *41*, 5809.
- [10] L. Di Maio, I. Coccorullo, *Macromol. Symp.* **2005**, *228*, 185.
- [11] M. Xanthos, C. Wan, *Polym. Int.* **2004**, *53*, 1161.
- [12] M. Xanthos, Q. Zhang, *J. Cell. Plast.* **1998**, *34*, 498.
- [13] S. V. Levchik, E. D. Weil, *Polym. Int.* **2005**, *54*, 11.
- [14] M. M. Velencoso, A. Battig, *Angew. Chem. Int. Ed.* **2018**, *57*, 10450.
- [15] S. D. Shaw, A. Blum, *Rev. Environ. Health* **2010**, *25*, 261.
- [16] J. Zhang, Q. Ji, *Polym. Degrad. Stab.* **2010**, *95*, 1211.
- [17] P. Müller, B. Schartel, *J. Appl. Polym. Sci.* **2016**, *133*, 1.
- [18] D. Goedderz, L. Weber, *J. Appl. Polym. Sci.* **2019**, *47876*, 1.
- [19] I. Gibson, M. F. Ashby, *Proc. R. Soc. Lond. A* **1982**, *382*, 43.
- [20] C. K. Lyon, V. H. Garrett, *J. Am. Oil Chem. Soc.* **1961**, *38*, 262.
- [21] M. Aksit, C. Zhao, *Polymers* **2019**, *11*, 268.
- [22] T. U. Patro, G. Harikishnan, *Polym. Eng. Sci.* **2008**, *48*, 1779.
- [23] J. Lobos, S. Velankar, *J. Cell. Plast.* **2016**, *52*, 57.
- [24] H. E. Naguib, C. B. Park, *J. Appl. Polym. Sci.* **2004**, *91*, 2661.
- [25] S. Doroudiani, C. B. Park, *Polym. Eng. Sci.* **1996**, *36*, 2645.
- [26] D. Raps, T. Köppl, *Polymer* **2014**, *55*, 1537.
- [27] H. Liu, C. Wang, W. Liu, *Cell. Polym.* **2014**, *33*, 189.
- [28] A. Firas, D. Pavel, *Eur. Polym. J.* **2005**, *41*, 1453.
- [29] L. Incarnato, P. Scarfato, *Polymer* **2000**, *41*, 6825.
- [30] B. Liu, Q. Xu, *J. Mater. Sci. Chem. Eng.* **2013**, *1*, 9.
- [31] A. Mehta, U. Gaur, *J. Polym. Sci.: Phys. Ed.* **1978**, *16*, 289.
- [32] Material Safety Datasheet, Albermarle Europe SPRL, Belgium, 2016.
- [33] Information on THOR flame retardant products and its properties. <https://www.thor.com/flameretardantsfilmsandtapes.html> (accessed: Nov. 2019).
- [34] Y. Zhang, B. Yu, *Ind. Eng. Chem. Res.* **2017**, *56*, 1245.
- [35] Material Safety Datasheet, Clariant Plastics & Coatings GmbH, Germany, 2017.
- [36] K. A. Salmeia, A. Goonie, *Polym. Degrad. Stab.* **2018**, *155*, 22.
- [37] S. N. Leung, A. Wong, *J. Appl. Polym. Sci.* **2008**, *108*, 3997.
- [38] A. Vannier, S. Duquesne, *Polym. Degrad. Stab.* **2008**, *93*, 818.
- [39] a) ISO 5660-1: Reaction-to-Fire Tests—Heat Release, Smoke Production and Mass Loss Rate—Part 1: Heat Release Rate (Cone Calorimeter Method), International Standard Organization, Geneva, Switzerland, 2002; b) ISO 5660-2: 2002. Reaction-to-Fire Tests—Heat Release, Smoke Production and Mass Loss Rate—Part 2: Smoke Production Rate (Dynamic Measurements) ISO, Geneva, Switzerland, 2002; c) ISO/TR 5660-3: 2003. Reaction-to-Fire Tests—Heat Release, Smoke Production and Mass Loss Rate—Part 3: Guidance on Measurement. ISO, Geneva, Switzerland, 2003.
- [40] B. Schartel, T. R. Hull, *Fire Mater.* **2007**, *31*, 327.

SUPPORTING INFORMATION

Additional supporting information may be found online in the Supporting Information section at the end of this article.

How to cite this article: Bethke C, Goedderz D, Weber L, Standau T, Döring M, Altstädt V. Improving the flame-retardant property of bottle-grade PET foam made by reactive foam extrusion. *J Appl Polym Sci.* 2020;137:e49042. <https://doi.org/10.1002/app.49042>